

Spin-independent effective mass in a valley-degenerate electron system

Suhas Gangadharaiah and Dmitrii L. Maslov

Department of Physics, University of Florida, P. O. Box 118440, Gainesville, FL 32611-8440

(Dated: February 8, 2020)

In a generic spin-polarized Fermi liquid, the masses of spin-up and spin-down electrons are expected to be different and to depend on the degree of polarization. This expectation is not confirmed by the experiments on two-dimensional heterostructures. We consider a model of an N -fold degenerate electron gas. It is shown that in the large- N limit, the mass is enhanced via a polaronic mechanism of emission/absorption of virtual plasmons. As plasmons are classical collective excitations, the resulting mass does not depend on N , and thus on polarization, to the leading order in $1/N$. We evaluate the $1/N$ corrections and show that they are small even for $N = 2$.

PACS numbers: 73.21.-b, 71.10.Ay, 71.18.+y, 71.10.Ca

The observation of an apparent metal-insulator transition in high-mobility Si metal-oxide-semiconductor-field-effect-transistors (MOSFET's) [1] challenged the scaling theory of localization [2], which predicts that a two-dimensional (2D) system undergoes only a continuous crossover between weak and strong localization regimes. Although there has been a substantial progress in understanding of transport and thermodynamic properties of MOSFET's and other heterostructures [3, 4], the origin of the observed phenomena is still a subject of discussion. Although a conventional (dirty) Fermi-liquid (FL) theory [5, 6] can account for many observed effects at least qualitatively and, in some cases, quantitatively, there is also a number of non-FL scenarios for the anomalous metallic state [7, 8]. On the experimental side, the main argument for the FL-nature of the metallic state is the observation of quite conventional Shubnikov-de Haas (ShdH) oscillations [3, 4], which implies an existence of well-defined quasiparticles albeit with the renormalized effective mass m^* and spin susceptibility χ_s^* . The ShdH and magnetoresistance experiments show that at low densities both m^* and χ_s^* are significantly enhanced compared to their band values [4] and, according to some studies [9, 10], even diverge at the resistive transition point.

Although none drastically non-FL features of the metallic state have been found in ShdH measurements as of now, there is one very intriguing observation which does seem to present a challenge for the FL theory, at least in its conventional formulation. Namely, in all studies when the spin and orbital degrees of freedom were controlled independently by applying a tilted magnetic field, the effective masses, m_{\uparrow}^* and m_{\downarrow}^* , and Dingle temperatures (impurity scattering rates), $T_{D\uparrow}$ and $T_{D\downarrow}$, of spin-up and -down electrons, were found to be almost the *same*. Moreover, m^* in MOSFETs [11, 12] was found to be independent of the spin polarization, whereas T_D was shown to depend on the polarization only weakly. In n-GaAs, the effective mass was found to depend on the parallel magnetic field [13]; however, this behavior was attributed to the coupling between the in- and out-of-plane degrees of freedom (Stern effect [14]), which is to

be expected in systems with wider quantum wells. Given that the Stern effect is subtracted off, the resulting dependence of m^* on the polarization is likely to be weak.

Why is this strange? Polarization is expected to lead to two effects: the spin-splitting of the effective mass, i.e., $m_{\uparrow}^* \neq m_{\downarrow}^*$, and dependences of both m_{\uparrow}^* and m_{\downarrow}^* on the polarization. The first effect can be understood by considering a partially spin-polarized FL as a two-component system. As the densities of the components are different, the corresponding couplings describing the interactions between the same and opposite spins are also different; hence *a priori* the mass renormalizations should also be different. That the masses should depend on polarization can be seen from considering two limiting cases: of zero- and full polarization. At fixed density n , the Fermi energy is doubled by fully polarizing the 2D system, hence the ratio of the Coulomb to Fermi energy $g \equiv e^2 \sqrt{\pi n} / E_F$ differs by a factor of 2 between the cases of zero and full polarization. The experiment shows that the mass does depend on the density; however, if g is the only dimensionless parameter that determines the mass renormalization, the same effect can be achieved by either varying n or by varying E_F via polarization at fixed n . Also, different Fermi velocities should result in different impurity scattering times for spin-up and -down electrons; hence the Dingle temperatures are also expected to be different. However, this is not what the experiment shows.

The qualitative arguments given above can be verified in a number of ways. Back in 1971, Overhauser predicted the spin-splitting and polarization dependence of m^* within the RPA approximation for the 3D case [15]. Repeating the calculation in 2D gives a similar result:

$$m_{\uparrow\downarrow}^*/m = 1 + \left(r_s / \sqrt{2\pi} \right) \ln r_s \mp \left(r_s \xi / 2\sqrt{2\pi} \right) \ln r_s, \quad (1)$$

where $\xi = (n_{\uparrow} - n_{\downarrow}) / (n_{\uparrow} + n_{\downarrow}) \ll 1$ is the polarization and $r_s = me^2 / \sqrt{\pi n}$. In the fully-polarized regime ($\xi = 1$), the spin-down electrons disappear, whereas the renormalization of m_{\uparrow}^* is by a factor of $\sqrt{2}$ smaller than for $\xi = 0$. This argument can be generalized for a (partially) spin-polarized FL [16], where the Landau interaction function has three independent components: $f^{\uparrow\uparrow}$,

$f^{\downarrow\downarrow}$, and $f^{\uparrow\downarrow} = f^{\downarrow\uparrow}$. The Galilean invariance then gives

$$\begin{aligned} m/m_{\uparrow}^* &= 1 - F_1^{\uparrow\uparrow} - (k_{F\downarrow}/k_{F\uparrow})F_1^{\uparrow\downarrow}; \\ m/m_{\downarrow}^* &= 1 - F_1^{\downarrow\downarrow} - (k_{F\uparrow}/k_{F\downarrow})F_1^{\downarrow\uparrow}, \end{aligned}$$

where $F_1^{ij} = m \int d\theta \cos \theta f^{ij}(\theta) / (2\pi)^2$, with $i, j = \uparrow, \downarrow$. Again, in general, $m_{\uparrow}^* \neq m_{\downarrow}^*$. In addition, the spin-splitting and polarization dependence of m^* are also obtained within the Gutzwiller approximation for the Hubbard model [17] (in this case, mass-splitting disappears at half-filling but the polarization dependence survives).

Absence of the polarization dependence of the effective mass suggests that m^* is renormalized via the interaction with some classical degree of freedom, which is not affected by the quantum degeneracy of the electron states. In this paper, we show such a mechanism may be provided by the interaction with (virtual) plasmons which dominate the mass renormalization beyond the weak-coupling regime. To this end, we turn to a model of a Coulomb gas with large degeneracy N , considered previously in Refs. [18], [19]. This model is relevant, first of all, to valley-degenerate systems, such as the (001) surface of a Si MOSFET, where $N = 4$ (two valleys and two spin projections). As the valley degeneracy plays a very important role in the dirty FL theory [5, 6] it is important to elucidate its role for the properties of a clean FL. However, the $1/N$ expansion turns out to be converging reasonably fast even for a non-valley degenerate system ($N = 2$) and, as such, it provides a simple yet non-trivial way of going beyond the weak-coupling limit for not too strong Coulomb interaction.

For a 2D N -fold degenerate Coulomb gas, the Fermi momentum is scaled down by a factor of $N^{-1/2}$ (since one has to distribute the same number of electrons among N isospin flavors), whereas the inverse screening radius (κ),

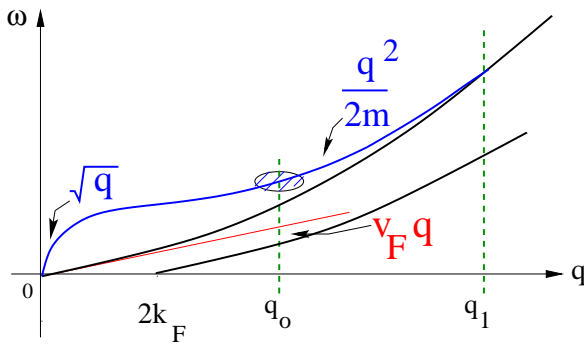


FIG. 1: Excitation spectrum for an N -fold degenerate 2D Coulomb gas in the strong-screening regime ($r_s N^{3/2} \gg 1$). The plasmon dispersion crosses over from the \sqrt{q} to q^2 form at $q \sim q_0 \sim r_s^{1/3} n^{1/2} \gg k_F$. Processes with momentum and energy transfers in the shaded oval ($q \sim q_0$ and $\omega \sim q_0^2/m$) dominate the mass enhancement. The plasmon spectrum merges with the continuum at $q = q_1 \sim r_s^{1/2} N^{1/4} n^{1/2} \gg q_0$.

proportional to the density of states, is scaled up by a factor of N . The ratio $\alpha \equiv \kappa/k_F = r_s N^{3/2}/2$ controls the crossover between the regimes of weak ($\alpha \ll 1$) and strong ($\alpha \gg 1$) screening. For $N \gg 1$, both of these regimes are compatible with the condition $r_s \ll 1$ which guarantees that the screening cloud includes many electrons, so that the mean-field theory is applicable. For $\alpha \ll 1$, the screening radius $\kappa^{-1} = \alpha^{-1} k_F^{-1}$ is larger than the Fermi wavelength. [This case also includes the usual RPA scheme for $N = 2$ —see Eq. (1).] The mass renormalization is mostly due to elastic scattering within the particle-hole continuum with momentum transfers $q \sim \kappa$, whereas the interaction with plasmons is small. In this regime, the mass depends on total degeneracy (N) and is thus strongly affected by polarization. Also, as scattering is mostly by small angles, $m^* < m$. For $\alpha \gg 1$, the effective screening radius $q_0^{-1} = (2\alpha)^{-1/3} k_F^{-1}$ is *smaller* than the Fermi wavelength (but still larger than the distance between electrons); hence, scattering is isotropic (*s*-wave). The particle-hole continuum contribution to m^* is greatly reduced for *s*-wave scattering, whereas the interaction with virtual plasmons now plays a dominant role. As the plasmon is a classical collective mode, it is not affected by a change in N . Consequently, the leading term in the N^{-1} expansion for m^* does not depend on N , whereas the next-to-leading term happens to be numerically small.

The effective mass is found from the self-energy via the usual relation (valid for a small renormalization)

$$m^*/m = 1 - \left(\frac{\partial \Delta \Sigma_k(\varepsilon)}{\partial \epsilon_k} + \frac{\partial \Delta \Sigma_k(\varepsilon)}{\partial (i\varepsilon)} \right) \Big|_{k \rightarrow k_F, \varepsilon \rightarrow 0},$$

where $\Delta \Sigma_k(\varepsilon) = \Sigma_k(\varepsilon) - \Sigma_{k_F}(0)$. It is convenient to separate $\Delta \Sigma_k(\varepsilon)$ into the static and dynamic parts as

$$\Delta \Sigma_k(\varepsilon) = \Delta \Sigma_k^{\text{st}}(\varepsilon) + \Delta \Sigma_k^{\text{dyn}}(\varepsilon), \quad (2)$$

where the static part for $\epsilon_k \equiv (k^2 - k_F^2)/2m \rightarrow 0$ is

$$\begin{aligned} \Delta \Sigma_k^{\text{st}}(\varepsilon) &= \int \frac{d\omega}{2\pi} \frac{d^2q}{(2\pi)^2} V_q(0) [G_{\mathbf{k}+\mathbf{q}}(\varepsilon + \omega) - G_{\mathbf{k}_F+\mathbf{q}}(\varepsilon)] \\ &= \frac{m}{(2\pi)^2} \epsilon_k \int_0^{2\pi} d\theta \cos \theta V_{2k_F \sin \theta/2}(0) \end{aligned} \quad (3)$$

with $G_{\mathbf{k}}^{-1}(\varepsilon) = i\varepsilon - \epsilon_k$ and

$$V_q(\omega) = [q/2\pi e^2 - \Pi_q(\omega)]^{-1}. \quad (4)$$

The dynamic part is

$$\begin{aligned} \Delta \Sigma_k^{\text{dyn}}(\varepsilon) &= \int \frac{d\omega}{2\pi} \frac{d^2q}{(2\pi)^2} [V_q(\omega) - V_q(0)] \\ &\quad \times [G_{\mathbf{k}+\mathbf{q}}(\varepsilon + \omega) - G_{\mathbf{k}_F+\mathbf{q}}(\varepsilon)]. \end{aligned} \quad (5)$$

In what follows, we will need the following two forms

of the polarization bubble

$$\begin{aligned} \Pi_q(\omega) &= N \int \frac{d\varepsilon}{2\pi} \int \frac{d^2k}{(2\pi)^2} G_{\mathbf{k}}(\varepsilon) G_{\mathbf{k}+\mathbf{q}}(\varepsilon + \omega) \quad (6) \\ &= - \begin{cases} (mN/2\pi) \left(1 - |\omega|/\sqrt{\omega^2 + v_F^2 q^2}\right), & \text{for } q \ll k_F; \\ 2n\varepsilon_q / (\varepsilon_q^2 + \omega^2), & \text{for } q \gg k_F, \end{cases} \end{aligned}$$

where $v_F = \sqrt{4\pi n/m^2 N}$ and $\varepsilon_q \equiv q^2/2m$.

In the weak-screening regime, $\Delta\Sigma_k^{\text{st}}(\varepsilon)$ [Eq. (2)] m^* gives the main contribution to m^* . To logarithmic accuracy, $m^*/m = 1 + (r_s \sqrt{N}/2\pi) \ln(r_s N^{3/2}) + \mathcal{O}(r_s)$ in this regime. [For $N = 2$ and $\xi = 0$, this reduces back to Eq. (1)]. In this regime, the plasmon contribution to m^* is a subleading, $\mathcal{O}(r_s)$ -term.

Now we turn to the strong-screening regime. The static screened potential in Eq. (3) is evaluated for $q = 2k_F \sin \theta/2 \leq 2k_F$. In this range, $V_q(0) = 2\pi e^2/(q + \kappa)$ is of the same form as in the weak-screening regime but now $V_q(0)$ depends on q only weakly because $q \ll \kappa$. Consequently, the angular averaging in Eq. (3) renders the static contribution to m^* small: $(m^*/m - 1)^{\text{st}} = 8/3\pi N\alpha$. Using the large- q form of Π in Eq. (6), one obtains $V_q(0) = 2\pi e^2 q^2 / (q^3 + q_0^3)$ for $q \gg k_F$, where $q_0 = (2\alpha)^{1/3} k_F \gg k_F$ is the inverse screening radius in this regime [19]. The main contribution to m^* comes from the region of large q and ω in Eq. (5), i.e., from the plasmon region. In the strong-screening regime, the plasmon dispersion is given by $\omega_p = \sqrt{\varepsilon_q^2 + 2\pi e^2 n q/m}$. The crossover between the \sqrt{q} and q^2 behaviors occurs at $q \sim q_0$. The plasmon runs into the continuum at $q \sim q_1 = k_F(\alpha/2)^{1/2} \gg q_0$. Most importantly, being the classical collective mode, plasmon is not affected by a change in N . The mass renormalization can be estimated as follows. Typical momenta and energy transfers are of the order of q_0 and ε_{q_0} , respectively; thus $V_{q_0}(\varepsilon_{q_0}) \sim e^2/q_0$, and $G \sim \omega^{-1} \sim \varepsilon_{q_0}^{-1}$. Combining these estimates together, one finds that $(m^*/m - 1)^{\text{dyn}} \sim \int d^2q \int d\omega V_q G^2 \sim r_s^{2/3}$, which is larger than the static contribution by $\alpha^{5/3} \gg 1$. To perform an actual calculation, we notice that the plasmon contribution from the region of large q to the effective mass can be written as

$$m^*/m = 1 + \frac{i}{\pi} \int_0^\infty d\varepsilon_q \text{Res} \frac{V_q(\omega)}{(i\omega - \varepsilon_q)^3} \Big|_{\omega=i\omega_p}, \quad (7)$$

where only the poles of $V_q(\omega)$ were taken into account, and where we have used the expansion $\epsilon_{\mathbf{k}+\mathbf{q}} = \epsilon_{\mathbf{k}} + v_F q \cos \theta (1 + \epsilon_{\mathbf{k}}/2E_F) + \varepsilon_q$. Substituting the large- q form of Π [Eq. (6)] into $V_q(\omega)$ in Eq. (7), one arrives at the result of Ref. [19] for the leading $1/N$ term in m^*

$$m^*/m = 1 + Cr_s^{2/3}, \quad (8)$$

where $C = \Gamma(1/3)\Gamma(1/6)/60\sqrt{\pi} \approx 0.14$.

Corrections to the leading term are obtained by including (a) interaction corrections to the bubble [Fig. 2(a)], (b) vertex correction to the self-energy [Fig. 2(b)], and (c) corrections to the polarization bubble from the small- q region. Estimating the diagrams in Fig. 2(a,b) in the same way as for the leading term, we find that both (a) and (b) contribute N -independent, $r_s^{4/3}$ corrections to Eq. (8). We have verified by an explicit calculation that these estimates do hold. Next, we consider correction (c) and show that it gives the next-to-leading term in the $1/N$ expansion.

The $1/q$ correction to the large- q form of the bubble [Eq. (6)] is

$$\delta\Pi_q(\omega) = \frac{4n^2\pi}{mN} \frac{(3\omega^2 - \varepsilon_q^2)\varepsilon_q^2}{(\omega^2 + \varepsilon_q^2)^3}. \quad (9)$$

At the plasmon pole ($\omega^2 = -\omega_p^2$) and for $q \sim q_0$, the relative correction $|\delta\Pi_q(\omega)/\Pi_q(\omega)| \sim 1/\alpha^{2/3}$, hence one can expect the next-to-leading term in the mass to be of order $r_s^{2/3}/\alpha^{2/3} \sim 1/N$. Indeed, a correction to the bubble (9) shifts the position of the plasmon-pole from ω_p^2 to $\omega_p^2 + \Delta^2$, where $\Delta^2 = 8\pi^2 n e^2 (3r^2 + 1)/Nmqr^4$ and $r = \sqrt{1 + (q_0/q)^3}$. Substituting this result into Eq. (7), and evaluating the q -integral to log-accuracy (the upper limit is determined by $q \sim q_1$, corresponding to the region where the plasmon runs into the continuum), we obtain m^* within the next-to-leading order in $1/N$ as

$$m^*/m = 1 + 0.14r_s^{2/3} + \frac{1}{12N} \log \left(r_s N^{3/2} \right) + \mathcal{O} \left(\frac{1}{r_s N^{5/2}} \right), \quad (10)$$

where the last term is the static contribution of the continuum. We see that the $1/N$ expansion generates the series in powers of $(r_s N^{3/2})^{-1}$.

Now we apply our main result, Eq. (10), to real systems. [In what follows, we neglect the last term in Eq. (10).] First of all, due to a small numerical coefficient in the leading term in Eq. (10), the actual constraint on r_s being small is rather soft: a two-fold enhancement of the mass occurs only for $r_s \approx 20$, hence smaller values of r_s still allows for a reasonable description within the mean-field theory. Eq. (10) agrees well with the observed dependence of $m^*(r_s)$ for Si MOSFETs in the range $r_s = 2 - 6$; for larger r_s , the theoretical value of m^* falls below the experimental one. In the interval $2 \leq r_s \leq 6$, the $1/N$ term in Eq. (10) is not that

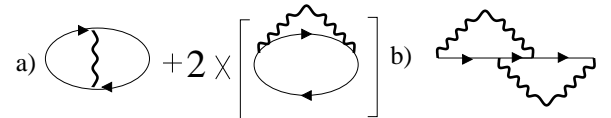


FIG. 2: a: corrections to the bubble; b: vertex correction to the self-energy.

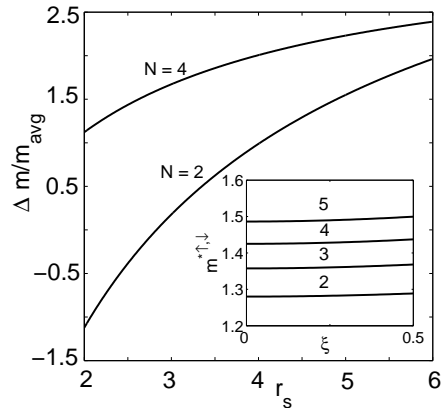


FIG. 3: Change in the effective mass under full spin polarization [cf. Eq. (11)], as a function of r_s . Inset: polarization dependence of the effective mass for $r_s = 2, 3, 4, 5$.

small: it constitutes 18-26 % and 26-32% of the leading term for $N = 4$ and $N = 2$, correspondingly. However, the relative change in m^* due to full spin polarization ($N \rightarrow N/2$)

$$\frac{\Delta m}{m_{\text{avg}}} = 2 \times \frac{m^*(N/2) - m^*(N)}{m^*(N/2) + m^*(N)} \times 100\%, \quad (11)$$

is small. $\Delta m/m_{\text{avg}}$ as a function of r_s is shown in Fig. 3 for $N = 4$ and $N = 2$. In both cases, these changes are less than 3 %, which is likely to be below the experimental error in the measured mass. At finite polarization, the result in Eq. (10) changes to

$$\frac{m_{\uparrow,\downarrow}^*}{m} = 1 + 0.14r_s^{2/3} + \frac{1 + \xi^2}{12N} \log \left[\frac{r_s N^{3/2}}{1 + \xi^2} \right]. \quad (12)$$

Notice that although an explicit polarization dependence does occur in the second term, there is no spin-splitting of the masses to this order in $1/N$. Eq. (12) is valid as long as there are still many spin-down electrons within the screening radius or, equivalently, $1 - \xi \gg r_s^{2/3} \sim (m^*/m - 1)$. Fig. 3 shows that the effective mass remains essentially constant in the whole range of ξ , which is in agreement with the experiment [12].

To leading order in $1/N$, the renormalization of χ^* is entirely due to that in m^* , so that $g^* = \chi^*/m^*$ remains unrenormalized [19]. We found that this remains true up to the next-to-leading term in $1/N$. This result is in qualitative agreement with the experiments on Si MOSFETs. However, recent experiment on AlAs system shows that the g^* factor is affected by lifting the valley degeneracy [20]. More work is required to attribute this behavior to a many-body effect.

Now, we comment briefly on the impurity scattering rate in the large- N limit. In the strong-screening regime, the screening radius (q_0^{-1}) is much larger than the Fermi wavelength. Therefore, scattering even on *charged* impurities is in the *s*-wave regime. We assume that the

main role is played by impurities within the 2D layer. Due to a peculiarity of 2D scattering [21], the scale of the scattering cross-section section is set by the wavelength (rather than by the impurity size $a \sim q_0^{-1}$) and depends on a weakly: $A \sim k_F^{-1} / \ln^2(k_F a)$. Consequently, the scattering rate $1/\tau = n_i v_F A$, where n_i is the concentration of impurities, has only a weak dependence on the polarization (via k_F under the logarithm). Thus $1/\tau$ (Dingle temperature) for spin-up and down-electrons are close to each other. Notice that both ShdH and weak-field Hall effect [22] show that $1/\tau$, while being the same for spin-up and spin-down electrons, increases strongly with r_s . Within our model, this can only be explained by an increase in the number of scatterers n_i with decreasing electron density—not an improbable scenario for Si MOSFETs.

Finally, we observe that as the mass is renormalized by plasmons with large q , the behavior of the plasmon spectrum at small q (gapped or gapless) is irrelevant. Consequently, in 3D the mass is renormalized in a similar way: $m^*/m = 1 + C_{3D} r_s^{3/4}$, where C_{3D} does not depend on N . Therefore, a finite thickness of the 2D layer should not affect the (approximate) spin-independence of the mass.

We aknowledge stimulating conversations with E. Abrahams, A. Chubukov, M. Fabrizio, M. Gershenson, A. Leggett, E. Mishchenko, V. Pudalov, M. Shayegan, and B. Spivak. This work was supported by NSF DMR-0308377.

- [1] S. V. Kravchenko, G. V. Kravchenko, J. E. Furneaux, V. M. Pudalov, and M. D'Iorio, Phys. Rev. B **50**, 8039 (1994).
- [2] E. Abrahams, P. W. Anderson, D. C. Licciardello, and T. V. Ramakrishnan, Phys. Rev. Lett. **42**, 673 (1979).
- [3] E. Abrahams, S. V. Kravchenko, and M. P. Sarachik, Rev. Mod. Phys. **73**, 251-266 (2001).
- [4] V. M. Pudalov, M. E. Gershenson, and H. Kojima, in *Fundamental Problems of Mesoscopic Physics. Interaction and Decoherence*, ed. by I. V. Lerner, B. L. Altshuler, and Y. Gefen, (Kluwer, 2004)
- [5] G. Zala, B. N. Narozhny, and I. L. Aleiner, Phys. Rev. B **65**, 020201(R) (2002).
- [6] A. Punnoose and A. M. Finkel'stein, Phys. Rev. Lett. **88**, 016802 (2002).
- [7] S. Chakravarty, L. Yin, and E. Abrahams, Phys. Rev. B **58**, R559-R562 (1998).
- [8] B. Spivak and S. A. Kivelson, Phys. Rev. B **70**, 155114 (2004); R. Jamei, S. Kivelson, and B. Spivak, Phys. Rev. Lett. **94**, 056805 (2005).
- [9] S. A. Vitkalov et al. Phys. Rev. Lett. **85**, 2164 (2000).
- [10] S. V. Kravchenko, A. A. Shashkin, D. A. Bloore, and T. M. Klapwijk, Solid State Commun. **116**, 495 (2000).
- [11] V. M. Pudalov, M. E. Gershenson, H. Kojima, N. Butch, E. M. Dizhur, G. Brunthaler, A. Prinz, and G. Bauer, Phys. Rev. Lett. **88**, 196404 (2002).
- [12] A. A. Shashkin et al. Phys. Rev. Lett. **91**, 046403 (2003).

- [13] E. Tutuc et al. Phys. Rev. B **67**, 241309(R) (2003).
- [14] F. Stern, Phys. Rev. Lett. **21**, 1687 (1968).
- [15] A. W. Overhauser, Phys. Rev. B **4**, 3318 (1971).
- [16] A. E. Meyerovich, J. Low. Temp. Phys. **53**, 487 (1983).
- [17] J. Spalek and P. Gopalan, Phys. Rev. Lett. **64**, 2823 (1990).
- [18] Y. Takada, Phys. Rev. B **43**, 5962-5978 (1991).
- [19] S. V. Iordanskii and A. Kashuba, JETP Lett. **76**, 563 (2002).
- [20] Y. P. Shkolnikov, K. Vakili, E. P. De Poortere, and M. Shayegan, Phys. Rev. Lett. **92**, 246804 (2004).
- [21] S. K. Adhikari, Am. J. Phys. **54**, 362 (1986).
- [22] S. A. Vitkalov, Phys. Rev. B **64**, 195336 (2001).